

## Human breast milk enhances intestinal mucosal barrier function and innate immunity in a pediatric human enteroid model

Gaelle Noel<sup>1#&</sup>, Julie G. In<sup>2, 3#</sup>, Jose M. Lemme-Dumit<sup>1#</sup>, Lauren R. DeVine<sup>4</sup>, Robert N. Cole<sup>4</sup>, Anthony L. Guerrero<sup>5</sup>, Olga Kovbasnjuk<sup>2,3\*</sup> and Marcela F. Pasetti<sup>1\*</sup>

<sup>1</sup>Department of Pediatrics, Center for Vaccine Development and Global Health, University of Maryland School of Medicine, Baltimore, MD.

<sup>2</sup>Department of Internal Medicine, Division of Gastroenterology and Hepatology, University of New Mexico Health Science Center, Albuquerque, NM.

<sup>3</sup>Department of Medicine, Division of Gastroenterology and Hepatology, Johns Hopkins University School of Medicine, Baltimore, MD.

<sup>4</sup>Department of Biological Chemistry, Johns Hopkins Mass Spectrometry and Proteomics Facility, Johns Hopkins University School of Medicine, Baltimore, MD.

<sup>5</sup>Department of Pediatrics, Johns Hopkins University School of Medicine, Baltimore, MD.

<sup>&</sup>Present address: Institut Pasteur, Center for Translational Science, 75015 Paris, France.

\*Corresponding authors

Marcela F. Pasetti; 685 West Baltimore St. Room 480, Baltimore, MD 21201. Phone: (410) 852-8957 E-mail: [mpasetti@som.umaryland.edu](mailto:mpasetti@som.umaryland.edu)

Olga Kobasnjuk; 1919 Lomas Blvd. NM 87106. Phone: (443) 791-8912 E-mail: [okovbasnjuk@salud.unm.edu](mailto:okovbasnjuk@salud.unm.edu)

#These authors contributed equally to this work

Conflict of Interest: The authors have declared that no conflict of interests exist.

1    **ABSTRACT**

2    Breastfeeding has been associated with long lasting health benefits. Nutrients and bioactive  
3    components of human breast milk promote cell growth, immune development, and shield the  
4    infant gut from insults and microbial threats. The molecular and cellular events involved in these  
5    processes are ill defined. We have established human pediatric enteroids and interrogated  
6    maternal milk's impact on epithelial cell maturation and function in comparison with commercial  
7    infant formula. Colostrum applied apically to pediatric enteroid monolayers reduced ion  
8    permeability, stimulated epithelial cell differentiation, and enhanced tight junction function by  
9    upregulating occludin expression. Breast milk heightened the production of antimicrobial peptide  
10     $\alpha$ -defensin 5 by goblet and Paneth cells, and modulated cytokine production, which abolished  
11    apical release of pro-inflammatory GM-CSF. These attributes were not found in commercial  
12    infant formula. Epithelial cells exposed to breast milk elevated apical and intracellular pIgR  
13    expression and enabled maternal IgA translocation. Proteomic data revealed a breast milk-  
14    induced molecular pattern associated with tissue remodeling and homeostasis. Using a novel *ex*  
15    *vivo* pediatric enteroid model, we have identified cellular and molecular pathways involved in  
16    human milk-mediated improvement of human intestinal physiology and immunity.

17

## 18 INTRODUCTION

19 The human gastrointestinal epithelium is a selective physical and chemical barrier that  
20 separates the luminal content from the serosal compartment and inner host tissues (1). It  
21 enables transport of electrolytes and nutrients, and provides a first line of defense against  
22 pathogens by engaging innate and adaptive mucosal immune components (2). The intestinal  
23 epithelium and associated mucosal immune environment progressively develop and mature  
24 from early fetal stages through childhood by means of genetic and external signals (3, 4).  
25 Human milk, rich in essential macronutrients, bioactive molecules (i.e., growth factors,  
26 antimicrobial peptides, complex oligosaccharides), and immune components including  
27 immunoglobulins, cytokines, and immune cells, supports tissue development and protects  
28 infants against infectious agents (5). Human milk is also a source of and helps establish a  
29 healthy microbiota in infants (6). Improvement of chronic and acute diseases (e.g., necrotizing  
30 enterocolitis, inflammatory bowel diseases, and intestinal and pulmonary infections) has been  
31 attributed to breastfeeding (7-10). Because of its countless benefits, breastfeeding has been  
32 recommended at least during the first 6 months of life (11). Current knowledge of the health-  
33 promoting benefits of human breast milk remains empiric or primarily descriptive, having been  
34 derived from observational or epidemiologic studies. The cellular and molecular mechanisms  
35 underlying the effects of maternal milk in the pediatric gut and physiologic pathways involved  
36 remain ill characterized. One of the reasons for this gap in knowledge is the lack of reliable  
37 models that could recapitulate the effect of human milk on the development and maintenance  
38 of a healthy pediatric human gut and its origin in modulating systemic effects. Studies using  
39 intestinal cancer cell lines including HT-29, T84, and Caco-2 cells or short-lived primary  
40 epithelial cells obtained from animals fail to reproduce the normal physiological responses of  
41 infant intestinal epithelium (12-15). Additionally, these immortalized cultures consist mainly of  
42 enterocytes and lack intestinal segment- and age-specificity needed for study of the complex  
43 multicellular and diverse composition of the human intestinal epithelium.

44 In this study, we described the establishment of an *ex vivo* pediatric human enteroid model  
45 derived from intestinal Lgr5<sup>+</sup> stem cells and a mechanistic interrogation of the effects of  
46 human breast milk in the intestinal epithelium. Human intestinal enteroids (HIEs) recapitulate  
47 the crypt-villus cell axis and the segment-specific physiology (duodenum, jejunum, ileum) of  
48 the adult human small intestine (16, 17). Technical advantages of HIEs include their capacity  
49 for long-term growth (years), which preserves donor genotype, and forming polarized  
50 monolayers with easy access to apical and basolateral epithelial cell surfaces, which avoids  
51 the cumbersome manipulation of 3D structures (18). Herein, we present a side-by-side  
52 comparison of the molecular and cellular events affected by human milk vs. commercial infant  
53 formula in human pediatric enteroids. Outcome analyses included pediatric intestinal tissue  
54 morphology and maturation, ion and epithelial barrier permeability, antimicrobial and immune  
55 functions, and epithelial cell secretome.

56

## 57 **RESULTS**

58 **Pediatric and adult enteroid monolayers exhibit distinct cell morphology and maturation**  
59 **features.** To mechanistically interrogate the physiological effects of human breast milk in the  
60 pediatric gut, differentiated enteroid monolayers were established from duodenal biopsies of  
61 healthy 2- and 5-year-old children who underwent diagnostic endoscopy at The Johns Hopkins  
62 Hospital, using methods previously described (19, 20); these monolayers are hereafter referred  
63 to as 2PD and 5PD, respectively. The cell morphology, permeability and barrier integrity of the  
64 pediatric monolayers were compared with those derived from adult duodenal tissue.  
65 Differentiated (villus-like) enterocytes of pediatric origin were significantly shorter than their adult  
66 counterparts as revealed by confocal microscopy images (Figure 1A) and epithelial cell height  
67 measurement (Figure 1B). Analysis of the epithelial barrier function by transepithelial electrical  
68 resistance (TER) revealed increased paracellular ion permeability in the pediatric- as compared  
69 to the adult-derived monolayers (Figure 1C).

70 **Human breast milk improves pediatric epithelial barrier function.** We next examined the  
71 effect of human breast milk (colostrum) on pediatric intestinal barrier function. Breast milk was  
72 applied to the apical side of differentiated pediatric enteroid monolayers, and TER values were  
73 monitored daily for 48h. Monolayers exposed to human breast milk exhibited higher TER values  
74 as compared to non-treated controls (Figures 2A and B). A dose-response effect was observed,  
75 with the 20% (v/v) treatment resulting in higher TER values as compared to 2% (v/v) (Figure  
76 2A). This observation was consistent in multiple experiments using both lines; the 20% (v/v)  
77 solution was therefore selected for subsequent experiments. We next compared ion  
78 permeability of pediatric monolayers treated with human milk vs. commercial infant formula  
79 (also resuspended at 20% w/v). Human breast milk significantly and reliably increased TER  
80 levels in both 2PD and 5PD monolayers as compared to non-treated controls and remained  
81 elevated or further improved with prolonged exposure (Figures 2A and B). By contrast, ion  
82 permeability was modestly affected by infant formula; TER values increased only in the 5PD  
83 monolayer at 48h of treatment (Figure 2B, right panel). In addition to transepithelial ion  
84 permeability by TER, paracellular molecular permeability was examined by exposing breast  
85 milk- and infant formula-treated pediatric monolayers to FITC-labelled 4kDa dextran for up to  
86 2h. No differences were observed in the amount of dextran recovered from the basolateral side  
87 regardless of treatment (data not shown) confirming integrity of the epithelial barrier.

88  
89 **Human breast milk increases the expression of the tight junction (TJ) protein occludin.**  
90 Maternal milk enhancement of TER values prompted us to investigate its effect on expression of  
91 TJ proteins, which seal the paracellular space of the intestinal epithelia and regulate passage of  
92 ions and small molecules. Occludin, a transmembrane protein of the TJ complex was selected  
93 for this analysis as crucial marker of epithelial differentiation and barrier function (21).  
94 Immunofluorescent imaging revealed occludin on the cell perimeter of all monolayers,  
95 regardless of treatment (Figure 3A). Strikingly, pediatric monolayers exposed to human milk

96 exhibited a distinctive pattern of apical and condensed cytoplasmic vesicular expression of  
97 occludin (Figure 3A) that markedly contrasted with the perimeter-only expression of monolayers  
98 treated with infant formula. Quantitative analysis of the fluorescence intensity by confocal  
99 imaging revealed superior occludin expression in both pediatric monolayers treated with human  
100 breast milk as compared with monolayers treated with infant formula or untreated controls  
101 (Figure 3B). Of the two enteroid lines, the 2PD was the higher and more consistent responder  
102 (Figure 3B). Infant formula increased occludin expression modestly and occasionally, not  
103 reaching significance above the non-treated controls (Figure 3B). The granular occludin  
104 expression pattern induced by breast milk was observed not only in absorptive enterocytes,  
105 visible by their prominent apical brush border, but also in cells lacking brush border, which are  
106 typically secretory epithelial cell lineages such as Paneth cells, goblet cells, and  
107 enteroendocrine cells (our HIE monolayers were not induced to express M cells). To identify the  
108 specific cell types producing occludin, breast milk-treated monolayers were co-stained to detect  
109 the presence of occludin as well as lysozyme, a marker for Paneth cells, trefoil factor 3 (TFF3),  
110 a marker for goblet cells, and chromogranin A, a marker for enteroendocrine cells. Occludin  
111 granular pattern co-localized with both lysozyme and TFF3, but not with chromogranin A marker  
112 (Figure 3C). These results indicate that breast milk elevates occludin expression not only at the  
113 TJ but also in the cytoplasm and apical membrane of absorptive enterocytes as well as in  
114 Paneth cells and goblet cells.

115  
116 **Human milk increases epithelial cell expression of innate immune mediators.** The  
117 influence of breast milk on Paneth cell protein expression led us to examine its capacity to  
118 enhance Paneth cell function, and in particular the production of antimicrobial peptides such as  
119  $\alpha$ -defensin 5 (DEFA5), which helps maintain intestinal tolerance and homeostasis (22, 23).  
120 DEFA5 fluorescence intensity was greatly increased in breast milk-treated pediatric monolayers  
121 as compared to those treated with infant formula or non-treated controls (Figures 4A and B).

122 Infant formula had no effect on DEFA5 expression. As expected, DEFA5 co-localized with  
123 lysozyme<sup>+</sup> Paneth cells (Figure 4B). Surprisingly, a subpopulation of DEFA5-expressing cells  
124 that lacked the lysozyme marker was observed in human milk-treated monolayers (Figure 4B).  
125 Dual DEFA5<sup>+</sup> and TFF3<sup>+</sup> fluorescent staining revealed co-localization of these two markers,  
126 uncovering a breast milk-induced human goblet cell population with capacity to produce DEFA5  
127 (Figure 4C).

128 We next examined the capacity of breast milk to modulate the production and secretion of  
129 cytokines and chemokines typically produced by intestinal epithelial cells. IL-10, IFN- $\gamma$ , TNF- $\alpha$ ,  
130 IL-6, IL-8, MCP-1, and GM-CSF were measured in the apical and basolateral milieu of treated  
131 and non-treated monolayers. IL-10 and IFN- $\gamma$  in all conditions were below limit of detection (<0.7  
132 pg). TNF- $\alpha$  and IL-6 were present at very low levels (<1 pg) and below the limit of detection in  
133 the non-treated controls, in both apical and basolateral compartments (data not shown). MCP-1,  
134 GM-CSF, and IL-8 were detected in apical media and for the most part, levels increased over  
135 time (Figures 4D-F). Treatment of pediatric monolayers with infant formula for 72h resulted in a  
136 marked increase of MCP-1 released apically as compared with non-treated monolayers. In  
137 contrast, a trend of reduced MCP-1 production was observed upon treatment with human milk  
138 (Figure 4D). GM-CSF was produced by untreated monolayers and by those treated with infant  
139 formula. In fact, infant formula produced a slight – yet not statistically significant – upregulation  
140 of GM-CSF at the 24h time point (Figure 4E). Conversely, apical GM-CSF secretion was  
141 abolished when monolayers were treated with human milk, at both time points tested (Figure  
142 4E). Apical release of IL-8 remained unaffected by treatment (Figure 4F). Basolateral secretion  
143 of MCP-1, GM-CSF, and IL-8 was not influenced by treatment either (data not shown). A  
144 principal component analysis (PCA) was conducted combining 24h outcomes described above to  
145 visualize, in aggregate, the impact of breast milk and infant formula on epithelial cell physiology  
146 (the 24h time point was selected because it allowed for a complete dataset for all treatments).

147 Monolayers untreated or exposed to infant formula clustered together and were largely distant  
148 from those exposed to breast milk by principal component 1 (Figure 4G). Breast milk treatment  
149 was associated with biomarkers of enhanced barrier function (DEFA5, occludin, and TER),  
150 whereas infant formula was linked to synthesis of pro-inflammatory cytokines (IL-8, MCP-1, and  
151 GM-CSF) (Figure 4G).

152

153 **Human milk sIgA translocates across pediatric enteroid monolayers.** Breast milk contains  
154 a variety of immune mediators, including antibodies that shield immunologically naïve infants  
155 from health threats. Maternal immunoglobulins, in particular sIgA, support infant immune  
156 development and regulation, enacting long lasting benefits. Early colostrum has high levels of  
157 maternal sIgA and IgG, and hence our system enabled us to investigate their interaction with  
158 pediatric intestinal epithelial cells. Both 2PD and 5PD monolayers expressed secretory  
159 component (SC) of the polymeric immunoglobulin receptor (pIgR), which mediates IgA  
160 translocation across the intestinal epithelium as well as the neonatal Fc receptor (FcRn),  
161 responsible for transepithelial IgG transport as shown by immunoblotting (Figures 5A and B).  
162 Confocal microscopy images revealed a diffuse cytoplasmic SC-pIgR expression in the non-  
163 treated controls, whereas epithelial cells exposed to breast milk exhibited not only intracellular  
164 but also basolateral and dense apical SC-pIgR expression (Figure 5A). Enhanced SC-pIgR  
165 expression in pediatric monolayers treated with breast milk was confirmed by immunoblotting  
166 (Figure 5C). Soluble SC-pIgR was detected in milk alone but not in infant formula (Figure 5C).  
167 We next compared apical to basolateral sIgA and IgG translocation in monolayers treated with  
168 breast milk vs. non-treated controls. Both sIgA and IgG were detected on basolateral side of  
169 milk-exposed epithelial cells; sIgA levels were significantly higher than those of the non-treated  
170 controls (Figure 5D).

171



172 **Breast milk-induced protein upregulation and basolateral secretion by pediatric epithelial**  
173 **cells.** The intestinal epithelium communicates with underlying tissues via secretion of nutrients,  
174 growth factors, cytokines, and regulatory peptides. Gut-derived molecules secreted to the  
175 basolateral compartment have the potential to disseminate systemically and act on remote  
176 tissues, exacting distant modulatory functions. To identify breast milk-induced molecules of  
177 intestinal origin that may have a wider (and possibly systemic) impact *in vivo*, we examined  
178 proteins secreted into the basolateral compartment of milk-exposed monolayers. Over 6000  
179 proteins were identified by a proteomic analysis. To select the differentially expressed proteins  
180 from a total of 392 secreted proteins (with high false discovery rate), we applied the cutoffs:  
181 adjusted p-value  $\leq 0.05$  and  $\log_2$  fold change at  $\pm 0.68$ . A total of 61 proteins had increased  
182 abundance in the breast milk-treated enteroids, whereas 21 were increased in the non-treated  
183 control (Figure 6A).

184 Proteins derived from human milk were found in the basolateral compartment of breast milk-  
185 treated monolayers, indicating apical to basolateral transepithelial translocation.

186 In addition, we observed increased levels of proteins related to mucosal protection and repair  
187 (e.g., TFF1-3, lysozyme C, amyloid-like protein), epithelial cell markers (e.g., EpCAM), growth  
188 factors (e.g., insulin-like growth factor-binding protein [IGFBP], fibroblast growth factor binding  
189 protein [FGFBP]), extracellular matrix remodeling proteins (e.g., metalloproteinase inhibitor  
190 proteins, basement membrane-specific heparan sulfate proteoglycan core protein) and cofactor  
191 carrier protein (e.g., transcobalamin 2) in the human breast milk-treated monolayers (Figure  
192 6A). In contrast, the non-treated monolayers exhibited increased expression of the  
193 apolipoprotein family, and annexin V (Figure 6A). The interactions among proteins with  
194 increased abundance in the breast milk-treated enteroids were examined using the STRING  
195 v11.0 database. The analysis revealed a significant protein-protein interaction ( $p\text{-value} < 1.0^{-16}$ )  
196 among 57 of them (228 edges), whereas 4 proteins showed no interactions within the network  
197 (Figure 6B). These results indicate that most of the proteins secreted by milk-exposed enteroids

198 do not act as independent entities but can deploy biological activity by either transient or stable  
199 association. A functional enrichment analysis was then performed utilizing the PANTHER and  
200 AMIGO2 classification database system to highlight the gene ontology (GO) terms annotated for  
201 cellular component, molecular function, and biological processes enriched within these protein  
202 sets (Figure 6C). The majority of the proteins were associated with the extracellular  
203 compartment (24.3%; GO:0044421, GO:0005576) as well as within the cell (12.1%;  
204 GO:0044464, GO:0005623) as constitutive protein with cytoplasmic or plasma membrane  
205 localization. The main molecular function identified was binding (51.4%; GO:0005488) followed  
206 by enzyme activity (28.6%; GO:0003824). In addition, these protein sets participate in multiple  
207 biological processes, including cell physiology, response to stimulus, metabolic functions, cell  
208 growth and maintenance, and immunity (Figure 6C).

209

## 210 **DISCUSSION**

211 Human breast milk is a rich source of nutrients and bioactive components that promote infant  
212 growth and immune development. In this work, using an *ex vivo* pediatric intestinal stem cell-  
213 derived human enteroid model, we have identified distinct protein synthesized and cellular  
214 functions modulated by human breast milk. HIEs represent a cutting-edge technology that  
215 recapitulates the structural and functional features of the human gastrointestinal tissue. They  
216 have been used to interrogate gut physiology, host responses to microbes, drug activity, and  
217 cell-to-cell communication (24-29). A side-by-side comparison of pediatric- vs. adult-derived  
218 duodenal HIE monolayers revealed age-associated differences with the former exhibiting  
219 shorter columnar epithelial cells and reduced TER, consistent with a less mature epithelial cell  
220 phenotype. Reduced enterocyte height has been reported in duodenal biopsies of infants, as  
221 compared to adult subjects (30). Together, these results suggest that intestinal epithelial cell  
222 development continues through childhood. They also demonstrate that age-specific cell  
223 morphology is preserved in the HIEs.

224 Several unique molecular events associated with human milk improvement of pediatric intestinal  
225 health were observed. The first was the ability of breast milk (colostrum) to enhance epithelial  
226 barrier function by reducing ion permeability and upregulating expression of the TJ complex  
227 regulator occludin. The breast milk-treated monolayers exhibited an unusual pattern of  
228 upregulated occludin protein expression. Occludin was detected not only at the (expected)  
229 intercellular junctions but also on the apical plasma membranes of absorptive enterocytes as  
230 well as Paneth and goblet cells. Condensed occludin-containing vesicles were spread  
231 intracellularly. Apical occludin localization has been reported recently in mouse organoids,  
232 primarily in intestinal stem cells and Paneth cells, and less abundantly in enterocytes and goblet  
233 cells, and its presence associated with reduced paracellular permeability (31). A regulatory  
234 mechanism that involves recruitment of occludin contained in cytoplasmic vesicles or in the  
235 apical plasma membrane (via differential phosphorylation) for TJ formation has been proposed  
236 (32); under this model, the extra junctional localization may represent protein reservoirs that  
237 enable prompt TJ formation required by dynamic metabolic and physiological processes. To the  
238 best of our knowledge, this is the first demonstration of apical and cytoplasmic multi-lamellar  
239 occludin expression by human pediatric intestinal cells upregulated in response to breast milk.

240 A second key observation was the capacity of human milk to substantially increase production  
241 of human DEFA5, a peptide that contributes to innate host defense against enteropathogens  
242 and promotes intestinal homeostasis by limiting inflammation and microbial translocation (22,  
243 33, 34). DEFA5 was produced not only by Paneth cells (the typical producers of antimicrobial  
244 molecules) but also by mucus-producing goblet cells. Production of DEFA5 by intestinal villous  
245 TFF3<sup>+</sup> (goblet cells) but not lysozyme<sup>+</sup> cells has been documented in human ileal biopsies (35).  
246 Goblet and Paneth cells derive from a common secretory cell progenitor under the regulation of  
247 ETS transcription factor Spdef (36). Lgr5<sup>+</sup> stem cells and Paneth cells are abundant in crypt-like,  
248 non-differentiated HIEs. The lifespan of Paneth cells in enteroids is approximately 30 days,  
249 regardless of differentiation, as was previously shown in adult differentiated 3D enteroids (16).

250 By contrast, the expression of DEFA5 in TFF3<sup>+</sup> goblet cells, which mark the differentiated small  
251 intestinal epithelium, is a new finding and may reflect a differentiating cell lineage stage  
252 prompted by breast milk-derived growth factors. The heightening production of TJ proteins and  
253 antimicrobial products induced by breast milk (but not infant formula) is consistent with the  
254 reported improved epithelial barrier of infants fed with breast milk over those fed by formula as  
255 determined by reduced ratio of lactulose-to-mannitol in urine (37).

256 A third important observation was the immune modulation associated with human milk treatment  
257 of pediatric epithelial cells. While infant formula increased the production of pro-inflammatory  
258 cytokines MCP-1 and GM-CSF, breast milk reduced MCP-1 levels and totally suppressed apical  
259 release of GM-CSF. Gut inflammatory diseases such as intestinal bowel disease and celiac  
260 disease coincide with elevated MCP-1 and GM-CSF in duodenal biopsies (38).

261 IL-8, an epithelial cell-derived neutrophil chemoattractant was produced by the pediatric  
262 intestinal epithelium. Although not overtly affected by treatment, IL-8 was associated with  
263 exposure to infant formula as shown by PCA analysis of early time-point outcomes. These  
264 results are consistent with the anti-inflammatory properties of human milk, which, in the pediatric  
265 gut are deployed by reducing or abolishing steady state levels of signals that may activate or  
266 recruit phagocytic cells and enhance pro-inflammatory cytokines (i.e., GM-CSF and MCP-1)  
267 (39).

268 Different from adult HIEs, the pediatric HIEs did not produce substantial levels of TGF- $\beta$ 1, IFN- $\gamma$ ,  
269 IL-6, and TNF- $\alpha$  (19); these findings suggest that beyond the immune modulation of maternal  
270 milk, the pediatric intestinal epithelium is intrinsically programmed to silence signals that trigger  
271 inflammatory processes.

272 Human milk's composition is complex and dynamic, and encompasses a vast diversity of  
273 soluble components that act as prebiotics, antiadhesives, antimicrobials, as well as molecules  
274 that affect cellular physiology, shield the host from inflammatory and pathogenic insults (40),

275 and promote healthy gut development. Bioactive components with attributed anti-inflammatory  
276 and homeostatic function in human milk include IL-10, TGF- $\beta$ , antioxidants, and enzymes such  
277 as lysozyme, glutathione peroxidase, and catalase (41). Additionally, human milk provides a  
278 variety of growth factors and tissue development/remodeling agents (42); proteomic analyses of  
279 human breast milk have been reported elsewhere (43, 44). We showed herein that many of  
280 these milk-derived components gain access to the subcellular space (see below). The exact  
281 molecules that trigger the effects described above and operatives, whether they work alone or in  
282 a synergistic/complementary manner, remain to be elucidated.

283 Maternal milk-derived sIgA provides an additional protective immune layer that excludes,  
284 neutralizes, and prevents microbial attachment to host cells (45). Mucosal dimeric IgA binds to  
285 pIgR on the basolateral surface of the epithelial cell membrane, is transported intracellularly and  
286 released at the apical surface, carrying a small portion of the pIgR-binding domain (46), the SC.  
287 Similar mechanism allows for IgM epithelial transport, whereas IgG employs the FcRn to  
288 bidirectionally cross epithelial tissues (47). Maternal antibodies provide antigen-specific  
289 defenses, support homeostasis, and promote infant immune development. In animal models,  
290 breast milk sIgA conferred long lasting benefits that included maintenance of a healthy  
291 microbiota and regulation of epithelial cell gene expression (48). A fourth relevant finding was  
292 the visualization of pIgR in the apical and basolateral membrane of breast milk-treated  
293 enterocytes. Breast milk itself contained an abundance of soluble SC-pIgR, but none was  
294 detected in commercial infant formula. The soluble SC-pIgR in maternal milk likely originates  
295 from maternal cellular debris. Free SC in human milk can bind enteric pathogens and toxins,  
296 and thus boosts non-specific host defenses (49) in the infant gut. We detected apical-to-basal  
297 sIgA transport in the maternal milk-exposed pediatric monolayers. This process supports  
298 intracellular pathogen neutralization and delivery of luminal antigens to lamina propria dendritic  
299 cells to induce tolerance or subepithelial phagocytic cells to imprint antigen specific immunity

300 (50). FcRn detection in the pediatric tissue confirms expression of this receptor beyond infancy.  
301 Others have reported FcRn being expressed in human intestinal epithelial cells (51, 52).  
302 We were unable to detect translocation of maternal IgG, despite this process being documented  
303 in animal models and cell lines (53). The variable localization of FcRn and pH requirements may  
304 restrict apical-to-basolateral transport while basolateral-to-apical appears to be more prevalent  
305 (54). Studies of FcRn distribution, IgG interaction and IgG immune complex translocation in  
306 pediatric HIEs are ongoing.

307 Beyond promoting a healthy gut, multiple and far reaching benefits have been attributed to  
308 human milk, including prevention of respiratory diseases, immune fitness, cognitive capacity,  
309 and overall physiological well-being (55) that endure into adolescence. Breast milk products  
310 released to the basal side of the epithelium could, conceivably, distribute systemically and  
311 thereby mediate long distant effects. Our proteomic analysis of breast milk-treated monolayers  
312 revealed a variety of molecules, some unique to breast milk, such as  $\alpha$ -lactalbumin,  $\beta$ -casein,  
313 and prolactin, which had evidently translocated across the monolayers, and others that were  
314 produced by the milk-exposed pediatric intestinal cells. For the latter, a complex network of  
315 interacting biomolecules was revealed, with diverse functions including those affecting growth  
316 factors, immune and antimicrobial activity, tissue structure, and homeostasis, which confirms  
317 the broad and pleiotropic nature of the processes affected by breast milk. The epithelial  
318 translocation of milk-derived proteins might have been facilitated by endocytosis of intact  
319 (undigested) molecules in our model. These proteins have health benefits by themselves. Milk  
320  $\alpha$ -lactalbumin, for example, shields soluble CD14 (sCD14) from proteolytic degradation (56),  
321 and sCD14 can bind lipopolysaccharide (LPS) and prevent inflammation and injury caused by  
322 soluble LPS or LPS-bearing organisms.  $\beta$ -casein is an immune modulator that regulates cell  
323 recruitment, ameliorates inflammation, and stimulates mucus production (57). Prolactin is a  
324 pleiotropic hormone that stimulates production of maternal milk. Expected benefits for the infant,

325 based on animal studies, include reduction of anxiety and stress and neurogenesis (58). In  
326 addition, osteopontin prevents inflammation and epithelial damage in mouse DSS-colitis model  
327 (59).

328 A variety of breast milk-upregulated tissue-derived proteins were identified, including the TFF  
329 family, which maintains and restores gut mucosal homeostasis and regulates complement  
330 activation via decay-accelerating factor, DAF (60); the amyloid-like protein, which participates in  
331 intestinal metabolic processes and modulates expression of MHC class I molecules (61, 62);  
332 and, insulin growth factor binding protein, fibroblast growth factor, basement membrane-specific  
333 heparan sulfate protein, and metalloproteinase inhibitor – all of which contribute to epithelial cell  
334 growth, tissue remodeling, and barrier integrity (63-65). Other secreted proteins included  
335 transcobalamin 2, which facilitates the transport of vitamin B12 within the organs (66) and  
336 epithelial cell adhesion molecule (EpCAM), which localizes in the basal cell membrane and  
337 facilitates cell-to-cell interaction and proliferation (67). Complement proteins (C3 and C4) were  
338 also present in the basal media from breast milk-treated enteroids; C4 participates in  
339 complement activation via the classical and lectin pathway, whereas C3 is a converging  
340 substrate for all activating pathways; C3 cleavage into C3a and C3b, along with C5 cleavage,  
341 trigger the rest of the complement cascade. C3, C4, and other complement components are  
342 present in human breast milk (43, 44). Likewise, human intestinal epithelial cells produce  
343 complement proteins (68, 69). The origin of the complement proteins we identified is unclear.  
344 We surmise they derive from breast milk because synthesis of complement proteins by the  
345 intestinal epithelial cells reportedly requires pro-inflammatory signals (downregulated by breast  
346 milk in our system) (70). Nonetheless, the fact that maternal complement molecules would  
347 trespass the pediatric epithelium is intriguing. Regardless of their source, complement can boost  
348 infant mucosal protective mechanisms (71).

349 Bovine colostrum has been shown to influence the proteome of HT-29 cells as well as epithelial  
350 cell glycosylation (72). We show, for the first time, that human milk influences the synthesis of  
351 multiple mediators of metabolic and physiologic functions that act locally or systemically.  
352 In summary, using a novel *ex vivo* pediatric HIE, several mechanisms associated with breast  
353 milk were identified that improve intestinal health: 1) cell differentiation and strengthening of the  
354 pediatric intestinal barrier by reduction of permeability and upregulation of TJ occludin with a  
355 unique expression pattern; 2) boosting of innate immunity by enhancing production of  
356 antimicrobial DEFA5 by Paneth and goblet cells; 3) immune modulation and passive  
357 immunization by increased production of pIgR and translocation of luminal sIgA; 4) reduction of  
358 pro-inflammatory cytokines; 5) translocation of breast milk proteins with anti-inflammatory and  
359 anti-microbial properties; and 6) expression of proteins responsible for tissue remodeling and  
360 mucosal homeostasis.

361

## 362 **Methods**

363 **Study approval.** Protocols for recruitment of human participants, obtaining informed consent,  
364 collecting and de-identifying biopsy samples were approved by the Johns Hopkins University  
365 School of Medicine (JHU SOM) Institutional Review Board (IRB) NA 00038329. Procedures for  
366 recruitment of mothers around delivery, obtaining informed consent and collection and de-  
367 identification of breast milk were approved under University of Maryland School of Medicine IRB  
368 HP-00065842.

369

370 **Generation of enteroid monolayers.** Duodenal biopsies were obtained from 5 healthy  
371 individuals, two pediatrics (ages 2, 5) and three adults (ages 25, 27, and 81 years) through  
372 endoscopy or surgical procedure. Enteroids were generated from Lgr5<sup>+</sup> intestinal crypts  
373 embedded in Matrigel (Corning, USA) in 24-well plates, as previously described (73). Enteroids  
374 were expanded in growth factor-enriched media containing Wnt3A, Rspo-1, and Noggin (18,



375 19). Multiple enteroid cultures were harvested with Cultrex Organoid Harvesting Solution  
376 (Trevigen, USA), fragmented and re-suspended in expansion media and seeded (100  $\mu$ l) on the  
377 inner surface of 0.4  $\mu$ m Transwell inserts (Corning, USA), pre-coated with human collagen IV  
378 (Sigma-Aldrich, USA), and 600  $\mu$ l of expansion media was added to the receiver plate well.  
379 Media was replenished every other day (20). Enteroid monolayer confluency was monitored by  
380 measuring TER, as previously described (20). Upon reaching confluency, monolayers were  
381 differentiated in media (DFM) free of Wnt3A and Rspo-1 for 5 days (20). All cultures were  
382 maintained at 37°C and 5% CO<sub>2</sub>.

383

384 **Breast milk preparation and monolayer treatment.** Human colostrum was obtained from  
385 women 0-3 days post-delivery. Commercial infant formula powder (Similac® Advance® Abbot  
386 Nutrition) was resuspended in sterile distilled water following manufacturer's instructions. Both  
387 human breast milk and infant formula suspensions were centrifuged twice (10 min each) at  
388 3,000g. The soluble fractions were extracted, aliquoted, and stored at -80°C until use. Enteroid  
389 monolayers were treated apically with 100  $\mu$ l of human milk or infant formula diluted 2 or 20% in  
390 DFM. Non-treated controls were treated with 100  $\mu$ l of DFM. TER was monitored daily while  
391 conducting experiments to ensure monolayer integrity.

392

393 **Dextran permeability assay.** FITC-labelled 4 kDa dextran (Millipore Sigma, St. Louis, MO;  
394 0.01% w/v in DFM) was added to the apical side of enteroid monolayers pre-treated with 20% of  
395 human milk or infant formula. Regular DFM (600  $\mu$ l) was added to the basolateral side.  
396 Basolateral media (100  $\mu$ l) was sampled at 30 min, 1 and 2h, and FITC-dextran content was  
397 measured by fluorescence intensity using an EnVision Multilabel Plate Reader (PerkinElmer,  
398 Waltham, MA). Sampled volume was replenished with fresh DFM.

399

400 **Immunofluorescence staining and confocal imaging.** Enteroid monolayers were fixed for 40  
401 min in 4% paraformaldehyde (Electron Microscopy Sciences, USA), washed with PBS for 10  
402 min, permeabilized and blocked for 1h with PBS containing 15% fetal bovine serum, 2% BSA,  
403 and 0.1% saponin, all at room temperature (RT). After washing with PBS, monolayers were  
404 incubated overnight at 4°C with primary antibodies (diluted 1:100 in PBS). The following primary  
405 antibodies (Ab) were used: occludin (mouse monoclonal [mAb], clone OC-3F10, Thermo Fisher  
406 Scientific), TFF3 (rabbit polyclonal [pAb], Millipore Sigma), lysozyme EC 3.2.1.17 (rabbit pAb,  
407 Dako), DEFA5 (mouse mAb, clone 8C8, Millipore Sigma), and SC-166 (mouse mAb provided by  
408 Dr. A. Hubbard, Johns Hopkins University School of Medicine). Stained monolayers were  
409 washed with PBS (3 times, 10 min each) and incubated with secondary antibodies (diluted  
410 1:100 in PBS) for 1h at RT. Secondary antibodies included goat anti-mouse Alexa Fluor-488 or  
411 -568, and goat anti-rabbit Alexa Fluor-488 or -568 (all Thermo Fisher Scientific). F-actin was  
412 detected by phalloidin Alexa Fluor-633, -647, or -568 (1:100; Thermo Fisher Scientific). Hoechst  
413 for nuclear/DNA labeling (Thermo Fisher Scientific) was used diluted 1:1000 in PBS. After  
414 incubation, cells were washed as described above, and mounted in FluorSave reagent (Millipore  
415 Sigma). Confocal images were taken using an LSM-510 META laser scanning confocal  
416 microscope (Zeiss, Germany) and ZEN 2012 imaging software (Zeiss) or BZ-X700 fluorescence  
417 microscope (Keyence, Japan) available through the Fluorescence Imaging Core of the Hopkins  
418 Basic Research Digestive Disease Development Center. For qualitative analysis, image settings  
419 were adjusted to optimize the signal. For quantitative analysis, the same settings were used  
420 across the samples, and protein-of-interest average intensity fluorescence was analyzed using  
421 MetaMorph software (Molecular Devices, CA).

422

423 **Protein extraction, immunoblotting, and proteomic analysis.** Enteroid monolayers were  
424 lysed in cold lysis buffer (60 mM HEPES pH 7.4, 150 mM KCl, 5 mM Na<sub>3</sub>EDTA, 5 mM EGTA, 1  
425 mM Na<sub>3</sub>VO<sub>4</sub>, 50 mM NaF, 2% SDS) supplemented with 1:100 of protease inhibitor cocktail

426 (P8340, Millipore Sigma). Lysis buffer was applied to the apical surface, and cells were scraped  
427 and sonicated on ice (3 times at 10 sec pulses each time using 30% energy input). The lysates  
428 were centrifuged 10 min at 14000 rpm at 4°C, and the supernatant containing soluble and  
429 membrane proteins was collected. Total protein concentration was determined using a DC  
430 protein assay (Bio-Rad, CA). Proteins were separated on Novex Wedgewell 4-20% gradient  
431 Tris-glycine gels (Life Technologies, CA) and transferred to nitrocellulose membranes. The  
432 following primary antibodies were used for immunoblotting: polyclonal rabbit anti-plgR (Abcam),  
433 monoclonal mouse anti-SC-166, and polyclonal rabbit anti-FcRn (Novus Biologicals) – all at a  
434 1:250 dilution, and mouse monoclonal anti-GAPDH (clone 6C5, Abcam) at 1:1000 dilution.  
435 Secondary antibodies included goat anti-mouse Alexa Fluor-488 or -568 and goat anti-rabbit  
436 Alexa Fluor-488 or -568 (Thermo Fisher Scientific). Western blots were processed using the  
437 iBind Flex device (Life Technologies, Carlsbad, CA) and then imaged on an Odyssey CLx  
438 imager (LI-COR, Lincoln, NE). Proteomic analysis was conducted on basolateral media from  
439 pediatric monolayers treated with human milk ( $n=3$ ) and non-treated control ( $n=2$ ) through the  
440 Mass Spectrometry and Proteomics Facility, Johns Hopkins University School of Medicine.

441  
442 **Cytokines/chemokines.** Cytokines and chemokines were quantified using commercial  
443 electrochemiluminescence microarray kits (Meso Scale Diagnostic, Rockville, MD) following the  
444 manufacturer's instructions. MCP-1, GM-CSF, and IL-8 levels were reported as the amount  
445 contained in the total volume of culture supernatant collected from the apical and basolateral  
446 side of the monolayers.

447  
448 **Statistics.** Statistical significances were calculated using the Student's *t*-test to compare two  
449 groups, or one-way-ANOVA with Šidák's or Tukey's post-test as appropriate among more than  
450 two groups. PCA was performed by selecting PC with eigenvalues greater than 1.0 (Kaiser

451 rule). Plots and statistical tests were performed using Prism software v9 (GraphPad, San Diego,  
452 CA). Differences were considered statistically significant at p-value  $\leq 0.05$ .

453

#### 454 **Author contributions**

455 GN, JGI, and JML-D conducted experiments and analyzed data; JML-D compiled final figures;  
456 LD and RC conducted proteomics analysis; AG obtained pediatric biopsies; OK and MFP  
457 conceptualized the study, secured funding, designed experiments and data analysis. All authors  
458 contributed to the writing and editing of the manuscript.

459

#### 460 **Acknowledgements**

461 This work was supported by a Grand Challenge Exploration award (Bill and Melinda Gates  
462 Foundation) OPP 1118529 and in part, by NIH grants R01AI117734 (to MFP), P01 AI125181 (to  
463 MFP and OK) and K01 DK106323 (JGI). The authors acknowledge the Integrated Physiology  
464 and Imaging Cores of the Hopkins Digestive Disease Basic and Translational Research Core  
465 Center (P30 DK089502) and the Johns Hopkins Mass Spectrometry and Proteomics Core.

## 466 REFERENCES

- 467 1. Zihni C, et al. Tight junctions: from simple barriers to multifunctional molecular gates.  
468 *Nat Rev Mol Cell Biol.* 2016;17(9):564-80.
- 469 2. Peterson LW, and Artis D. Intestinal epithelial cells: regulators of barrier function and  
470 immune homeostasis. *Nat Rev Immunol.* 2014;14(3):141-53.
- 471 3. Torow N, et al. Neonatal mucosal immunology. *Mucosal Immunol.* 2017;10(1):5-17.
- 472 4. Stras SF, et al. Maturation of the Human Intestinal Immune System Occurs Early in Fetal  
473 Development. *Dev Cell.* 2019;51(3):357-73 e5.
- 474 5. Turfkruyer M, and Verhasselt V. Breast milk and its impact on maturation of the  
475 neonatal immune system. *Curr Opin Infect Dis.* 2015;28(3):199-206.
- 476 6. Ballard O, and Morrow AL. Human milk composition: nutrients and bioactive factors.  
477 *Pediatr Clin North Am.* 2013;60(1):49-74.
- 478 7. Bode L. Human Milk Oligosaccharides in the Prevention of Necrotizing Enterocolitis: A  
479 Journey From in vitro and in vivo Models to Mother-Infant Cohort Studies. *Front Pediatr.*  
480 2018;6:385.
- 481 8. Jantscher-Krenn E, et al. The human milk oligosaccharide disialyllacto-N-tetraose  
482 prevents necrotising enterocolitis in neonatal rats. *Gut.* 2012;61(10):1417-25.
- 483 9. Barclay AR, et al. Systematic review: the role of breastfeeding in the development of  
484 pediatric inflammatory bowel disease. *J Pediatr.* 2009;155(3):421-6.
- 485 10. Oddy WH. Breastfeeding, Childhood Asthma, and Allergic Disease. *Ann Nutr Metab.*  
486 2017;70 Suppl 2:26-36.
- 487 11. World Health Organization. *WHO Recommendations on Postnatal Care of the Mother  
488 and Newborn.* Geneva; 2013.
- 489 12. Sun D, et al. Comparison of human duodenum and Caco-2 gene expression profiles for  
490 12,000 gene sequences tags and correlation with permeability of 26 drugs. *Pharm Res.*  
491 2002;19(10):1400-16.
- 492 13. Drummond CG, et al. Enteroviruses infect human enteroids and induce antiviral  
493 signaling in a cell lineage-specific manner. *Proc Natl Acad Sci U S A.* 2017;114(7):1672-7.
- 494 14. Lin S, et al. Comparison of the transcriptional landscapes between human and mouse  
495 tissues. *Proc Natl Acad Sci U S A.* 2014;111(48):17224-9.
- 496 15. Pulendran B, and Davis MM. The science and medicine of human immunology. *Science.*  
497 2020;369(6511).
- 498 16. Sato T, et al. Single Lgr5 stem cells build crypt-villus structures in vitro without a  
499 mesenchymal niche. *Nature.* 2009;459(7244):262-5.
- 500 17. Zachos NC, et al. Human Enteroids/Colonoids and Intestinal Organoids Functionally  
501 Recapitulate Normal Intestinal Physiology and Pathophysiology. *J Biol Chem.*  
502 2016;291(8):3759-66.
- 503 18. In JG, et al. Human colonoid monolayers to study interactions between pathogens,  
504 commensals, and host intestinal epithelium. *J Vis Exp.* 2019(146).
- 505 19. Noel G, et al. A primary human macrophage-enteroid co-culture model to investigate  
506 mucosal gut physiology and host-pathogen interactions. *Sci Rep.* 2017;7:45270.
- 507 20. Staab JF, et al. Co-Culture System of Human Enteroids/Colonoids with Innate Immune  
508 Cells. *Curr Protoc Immunol.* 2020;131(1):e113.

- 509 21. Al-Sadi R, et al. Occludin regulates macromolecule flux across the intestinal epithelial  
510 tight junction barrier. *Am J Physiol Gastrointest Liver Physiol*. 2011;300(6):G1054-64.
- 511 22. Bevins CL, and Salzman NH. Paneth cells, antimicrobial peptides and maintenance of  
512 intestinal homeostasis. *Nat Rev Microbiol*. 2011;9(5):356-68.
- 513 23. Sankaran-Walters S, et al. Guardians of the Gut: Enteric Defensins. *Front Microbiol*.  
514 2017;8:647.
- 515 24. In JG, et al. Epithelial WNT2B and Desert Hedgehog Are Necessary for Human Colonoid  
516 Regeneration after Bacterial Cytotoxin Injury. *iScience*. 2020;23(10):101618.
- 517 25. Liu L, et al. Mucus layer modeling of human colonoids during infection with  
518 enteroaggregative *E. coli*. *Sci Rep*. 2020;10(1):10533.
- 519 26. Co JY, et al. Controlling epithelial polarity: A human enteroid model for host-pathogen  
520 interactions. *Cell Rep*. 2019;26(9):2509-20.e4.
- 521 27. King AJ, et al. Inhibition of sodium/hydrogen exchanger 3 in the gastrointestinal tract by  
522 tenapanor reduces paracellular phosphate permeability. *Sci Transl Med*. 2018;10(456).
- 523 28. Lin SC, et al. Human norovirus exhibits strain-specific sensitivity to host interferon  
524 pathways in human intestinal enteroids. *Proc Natl Acad Sci U S A*. 2020;117(38):23782-  
525 93.
- 526 29. Chang-Graham AL, et al. Rotavirus induces intercellular calcium waves through ADP  
527 signaling. *Science*. 2020;370(6519).
- 528 30. Thompson FM, et al. Epithelial growth of the small intestine in human infants. *J Pediatr*  
529 *Gastroenterol Nutr*. 1998;26(5):506-12.
- 530 31. Pearce SC, et al. Marked differences in tight junction composition and macromolecular  
531 permeability among different intestinal cell types. *BMC Biol*. 2018;16(1):19.
- 532 32. Wong V. Phosphorylation of occludin correlates with occludin localization and function  
533 at the tight junction. *Am J Physiol*. 1997;273(6):C1859-67.
- 534 33. Salzman NH, et al. Enteric defensins are essential regulators of intestinal microbial  
535 ecology. *Nat Immunol*. 2010;11(1):76-83.
- 536 34. Ehmann D, et al. Paneth cell alpha-defensins HD-5 and HD-6 display differential  
537 degradation into active antimicrobial fragments. *Proc Natl Acad Sci U S A*.  
538 2019;116(9):3746-51.
- 539 35. Cunliffe RN, et al. Human defensin 5 is stored in precursor form in normal Paneth cells  
540 and is expressed by some villous epithelial cells and by metaplastic Paneth cells in the  
541 colon in inflammatory bowel disease. *Gut*. 2001;48(2):176-85.
- 542 36. Gregorieff A, et al. The ets-domain transcription factor Spdef promotes maturation of  
543 goblet and paneth cells in the intestinal epithelium. *Gastroenterology*.  
544 2009;137(4):1333-45 e1-3.
- 545 37. Catassi C, et al. Intestinal permeability changes during the first month: effect of natural  
546 versus artificial feeding. *J Pediatr Gastroenterol Nutr*. 1995;21(4):383-6.
- 547 38. Di Sabatino A, et al. Innate and adaptive immunity in self-reported nonceliac gluten  
548 sensitivity versus celiac disease. *Dig Liver Dis*. 2016;48(7):745-52.
- 549 39. Hamilton JA. GM-CSF in inflammation. *J Exp Med*. 2020;217(1).
- 550 40. Bode L. The functional biology of human milk oligosaccharides. *Early Hum Dev*.  
551 2015;91(11):619-22.

- 552 41. Cacho NT, and Lawrence RM. Innate Immunity and Breast Milk. *Front Immunol.*  
553 2017;8:584.
- 554 42. Ogra PL. Immunology of Human Milk and Lactation: Historical Overview. *Nestle Nutr Inst*  
555 *Workshop Ser.* 2020;94:11-26.
- 556 43. Zhu J, and Dingess KA. The Functional Power of the Human Milk Proteome. *Nutrients.*  
557 2019;11(8).
- 558 44. Gao X, et al. Temporal changes in milk proteomes reveal developing milk functions. *J*  
559 *Proteome Res.* 2012;11(7):3897-907.
- 560 45. Cerutti A, and Rescigno M. The biology of intestinal immunoglobulin A responses.  
561 *Immunity.* 2008;28(6):740-50.
- 562 46. Brandtzaeg P. Secretory IgA: Designed for Anti-Microbial Defense. *Front Immunol.*  
563 2013;4:222.
- 564 47. Pyzik M, et al. FcRn: The Architect Behind the Immune and Nonimmune Functions of IgG  
565 and Albumin. *J Immunol.* 2015;194(10):4595-603.
- 566 48. Rogier EW, et al. Secretory antibodies in breast milk promote long-term intestinal  
567 homeostasis by regulating the gut microbiota and host gene expression. *Proc Natl Acad*  
568 *Sci U S A.* 2014;111(8):3074-9.
- 569 49. Giugliano LG, et al. Free secretory component and lactoferrin of human milk inhibit the  
570 adhesion of enterotoxigenic Escherichia coli. *J Med Microbiol.* 1995;42(1):3-9.
- 571 50. Corthesy B. Multi-faceted functions of secretory IgA at mucosal surfaces. *Front*  
572 *Immunol.* 2013;4:185.
- 573 51. Israel EJ, et al. Expression of the neonatal Fc receptor, FcRn, on human intestinal  
574 epithelial cells. *Immunology.* 1997;92(1):69-74.
- 575 52. Latvala S, et al. Distribution of FcRn Across Species and Tissues. *J Histochem Cytochem.*  
576 2017;65(6):321-33.
- 577 53. Dickinson BL, et al. Bidirectional FcRn-dependent IgG transport in a polarized human  
578 intestinal epithelial cell line. *J Clin Invest.* 1999;104(7):903-11.
- 579 54. Aaen KH, et al. The neonatal Fc receptor in mucosal immune regulation. *Scand J*  
580 *Immunol.* 2021;93(2):e13017.
- 581 55. Krol KM, and Grossmann T. Psychological effects of breastfeeding on children and  
582 mothers. *Bundesgesundheitsblatt Gesundheitsforschung Gesundheitsschutz.*  
583 2018;61(8):977-85.
- 584 56. Spencer WJ, et al. Alpha-lactalbumin in human milk alters the proteolytic degradation of  
585 soluble CD14 by forming a complex. *Pediatr Res.* 2010;68(6):490-3.
- 586 57. Chatterton DE, et al. Anti-inflammatory mechanisms of bioactive milk proteins in the  
587 intestine of newborns. *Int J Biochem Cell Biol.* 2013;45(8):1730-47.
- 588 58. Torner L. Actions of Prolactin in the Brain: From Physiological Adaptations to Stress and  
589 Neurogenesis to Psychopathology. *Front Endocrinol (Lausanne).* 2016;7:25.
- 590 59. Woo SH, et al. Osteopontin Protects Colonic Mucosa from Dextran Sodium Sulfate-  
591 Induced Acute Colitis in Mice by Regulating Junctional Distribution of Occludin. *Dig Dis*  
592 *Sci.* 2019;64(2):421-31.
- 593 60. Andoh A, et al. Intestinal trefoil factor induces decay-accelerating factor expression and  
594 enhances the protective activities against complement activation in intestinal epithelial  
595 cells. *J Immunol.* 2001;167(7):3887-93.

- 596 61. Puig KL, et al. Amyloid precursor protein mediated changes in intestinal epithelial  
597 phenotype in vitro. *PLoS One*. 2015;10(3):e0119534.
- 598 62. Tuli A, et al. Amyloid precursor-like protein 2 increases the endocytosis, instability, and  
599 turnover of the H2-K(d) MHC class I molecule. *J Immunol*. 2008;181(3):1978-87.
- 600 63. Austin K, et al. IGF binding protein-4 is required for the growth effects of glucagon-like  
601 peptide-2 in murine intestine. *Endocrinology*. 2015;156(2):429-36.
- 602 64. Tassi E, et al. Impact of fibroblast growth factor-binding protein-1 expression on  
603 angiogenesis and wound healing. *Am J Pathol*. 2011;179(5):2220-32.
- 604 65. Cabral-Pacheco GA, et al. The Roles of Matrix Metalloproteinases and Their Inhibitors in  
605 Human Diseases. *Int J Mol Sci*. 2020;21(24).
- 606 66. Quadros EV, et al. Transcobalamin II synthesized in the intestinal villi facilitates transfer  
607 of cobalamin to the portal blood. *Am J Physiol*. 1999;277(1):G161-6.
- 608 67. Das B, et al. Enteroids expressing a disease-associated mutant of EpCAM are a model for  
609 congenital tufting enteropathy. *Am J Physiol Gastrointest Liver Physiol*.  
610 2019;317(5):G580-G91.
- 611 68. Moon R, et al. Complement C3 production in human intestinal epithelial cells is  
612 regulated by interleukin 1beta and tumor necrosis factor alpha. *Arch Surg*.  
613 1997;132(12):1289-93.
- 614 69. Kopp ZA, et al. Do antimicrobial peptides and complement collaborate in the intestinal  
615 mucosa? *Front Immunol*. 2015;6:17.
- 616 70. Andoh A, et al. Differential cytokine regulation of complement C3, C4, and factor B  
617 synthesis in human intestinal epithelial cell line, Caco-2. *J Immunol*. 1993;151(8):4239-  
618 47.
- 619 71. Ogundele M. Role and significance of the complement system in mucosal immunity:  
620 particular reference to the human breast milk complement. *Immunol Cell Biol*.  
621 2001;79(1):1-10.
- 622 72. Morrin ST, et al. Interrogation of Milk-Driven Changes to the Proteome of Intestinal  
623 Epithelial Cells by Integrated Proteomics and Glycomics. *J Agric Food Chem*.  
624 2019;67(7):1902-17.
- 625 73. Sato T, et al. Long-term expansion of epithelial organoids from human colon, adenoma,  
626 adenocarcinoma, and Barrett's epithelium. *Gastroenterology*. 2011;141(5):1762-72.

627

## 628 **Figure legends**

### 629 **Figure 1. Pediatric and adult enteroid monolayers exhibit distinct maturation features. (A)**

630 Confocal microscopy images (XZ projections) depicting the difference in epithelial cell height  
631 between pediatric and adult enteroid monolayers. Actin, magenta; DNA, blue. Scale bar=20  $\mu$ m.

632 **(B)** Epithelial cell heights quantified by immunofluorescent confocal microscopy analysis ( $\geq 8$

633 different view fields). **(C)** TER values of enteroid monolayers. Images are representative of three



634 independent experiments (A). Data shown in (B) and (C) represent the mean  $\pm$  SEM from three  
635 (B) or two (C) independent experiments that included  $n=8-12$  enteroid monolayers/group per  
636 experiment. Each symbol represents an independent monolayer. (A-C) All measurements  
637 included 2 pediatric- and 3 adult-derived monolayers. (B, C) p-values were calculated by  
638 Student's *t* test.

639

640 **Figure 2. Human milk decreases ion permeability of the pediatric intestinal epithelium.**

641 (A) TER values of 2PD monolayers apically treated with 2% or 20% (v/v) of human milk (HM).  
642 (B) TER measurement of 2PD and 5PD monolayers apically treated with 20% (v/v) of HM or  
643 20% (w/v) of commercial infant formula. Mean  $\pm$  SEM. are shown. Data are representative of  
644 three independent experiments with  $n=3-6$  enteroid monolayers/group per experiment. p-values  
645 were calculated by one-way-ANOVA with Šidák's post-hoc analysis. Unless indicated, p-values  
646 correspond to treated vs. non-treated controls.

647

648 **Figure 3. Human milk modulates occludin expression.** (A) Confocal microscopy images (XY

649 and YZ projections) of 2PD enteroid monolayers untreated (NT) or apically treated for 24h with  
650 HM (20%; v/v) or IF (20%; w/v). Occludin, green; actin, magenta. Scale bar=10  $\mu$ m. (B) Relative  
651 fluorescence intensity of occludin quantified by confocal microscopy analysis of 2PD (left) and  
652 5PD (right) monolayers treated with HM (20%; v/v) or IF (20%; w/v) for 24h and 72h. Mean  $\pm$   
653 SEM are shown. Data are pooled from three independents with  $n=4-6$  enteroid  
654 monolayers/group per experiment. Each symbol indicates an independent monolayer. p-values  
655 were calculated by one-way-ANOVA with Šidák's post-hoc analysis. (C) Confocal microscopy  
656 images (XY projections) of 5PD enteroid monolayers treated with HM for 48h. Occludin, green;  
657 lysozyme (Lyz; XY projection), red; trefoil factor 3 (TFF3; XY projection), red; chromogranin A  
658 (ChgA; XY and XZ projections), red; actin, magenta; DNA, blue. Paneth and goblet cells, scale

659 bar=5  $\mu\text{m}$ ; enteroendocrine cells, scale bar=10  $\mu\text{m}$ . (A and C) Data are representative of three  
660 independent experiments with  $n=3$  enteroid monolayers/group per experiment.

661  
662 **Figure 4. Human milk modulates epithelial innate immune mediators.** (A) Relative  
663 fluorescence intensity of human DEFA5 quantified by confocal microscopy analysis of 2PD and  
664 5PD monolayers NT or treated with HM (20%; v/v) or IF (20%; w/v) for 48h. (B) Representative  
665 confocal microscopy images (XY projections) of 5PD monolayer showing localization  
666 (arrowheads) of DEFA5 in Lyz<sup>+</sup> cells in HM-treated monolayer. DEFA5, green; Lyz, red; actin,  
667 magenta; DNA, blue. Scale bar=10  $\mu\text{m}$ . (C) Representative confocal microscopy images (XY  
668 projections) of 5PD monolayer depicting co-localization (arrowheads) of TFF3 (red) and DEFA5  
669 (green); DNA, blue. Scale bar=50  $\mu\text{m}$ . (D-F) Total amount of MCP-1, GM-CSF, and IL-8 in the  
670 apical media of 2PD monolayer treated as described in (A) for 24h and 72h. (G) PCA plot from  
671 HM-, and IF-treated, and NT enteroid monolayers for 24h. PC, principal component. Variables  
672 analyzed: TER, occludin, DEFA5, MCP-1, GM-CSF, IL-8. (A, D-F). Mean  $\pm$  SEM are shown.  
673 Data are representative of three independent experiments with  $n=6-12$  enteroid  
674 monolayers/group per experiment. Each symbol indicates an independent monolayer. p-values  
675 were calculated by one-way-ANOVA with Tukey's post-test for multiple comparisons.

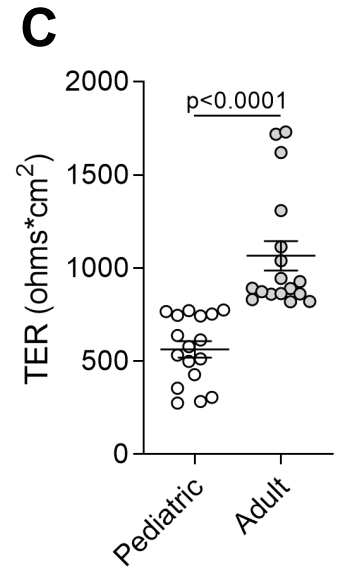
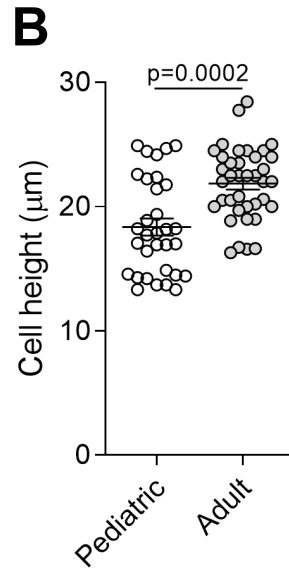
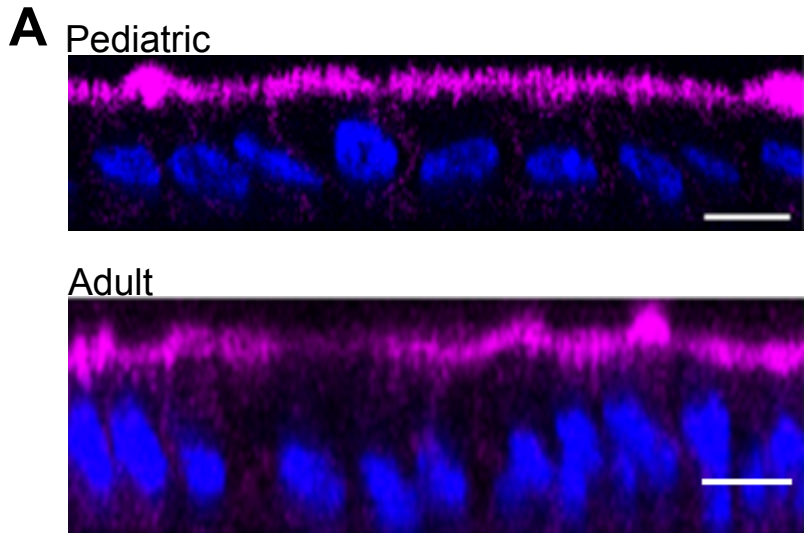
676  
677 **Figure 5. Breast milk enhances expression of pIgR and sIgA translocation across the**  
678 **epithelial monolayers.** (A) Confocal microscopy images showing SC (left, XZ projections,  
679 scale bar=10  $\mu\text{m}$ ; right, XY projection, scale bar=5  $\mu\text{m}$ ) in 5PD enteroid monolayer NT or treated  
680 with 20% (v/v) of HM for 72h. SC, green; actin, red; DNA, blue. (B) Composite immunoblotting  
681 (IB) showing SC and FcRn expression in non-treated 2PD and 5PD monolayers. (C) IB showing  
682 pIgR expression in HM and IF, and 2PD monolayers NT or treated with 20% (v/v) HM. MW,  
683 molecular weight. (D) Total IgA and IgG in the basolateral media of pediatric monolayers treated

684 for 48h with 20% (v/v) HM. Data represent mean  $\pm$  SEM of three combined experiments, each  
685 including 2 monolayers/group per experiment. Each symbol indicates an independent  
686 monolayer. p-value was calculated by Student's *t* test.

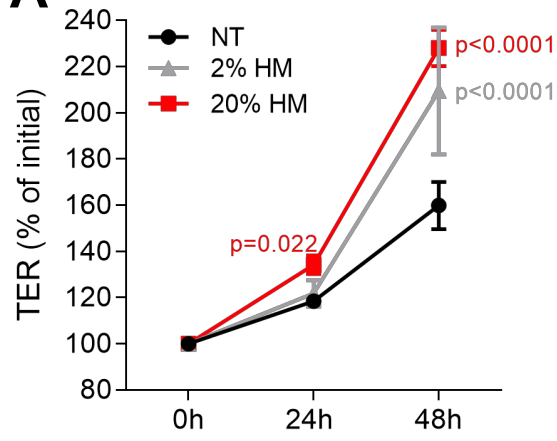
687

688 **Figure 6. Human milk modifies epithelial cell protein expression and basolateral**  
689 **secretion.** (A) Volcano plot of differential protein abundance (high false discovery rate) in the  
690 basolateral culture supernatant of 2PD monolayers NT ( $n=2$ ) or treated with 20% HM (v/v) ( $n=3$ )  
691 for 24h. Red dots indicate HM unique proteins; blue dots indicate epithelial cell-derived proteins;  
692 green dots indicate proteins derived from both HM and epithelial cells. (B) Protein-protein  
693 interaction analysis of 61 upregulated proteins produced by HM-treated monolayers selected  
694 based on the cut off shown in (A). Medium confidence interaction score = 0.400. A thicker line  
695 between nodes indicates stronger protein-protein interaction. (C) Enrichment analysis of GO  
696 terms annotated for cellular component, molecular function, and biological process of the 61  
697 upregulated proteins as described in (A).

# Figure 1



**A**



**B**

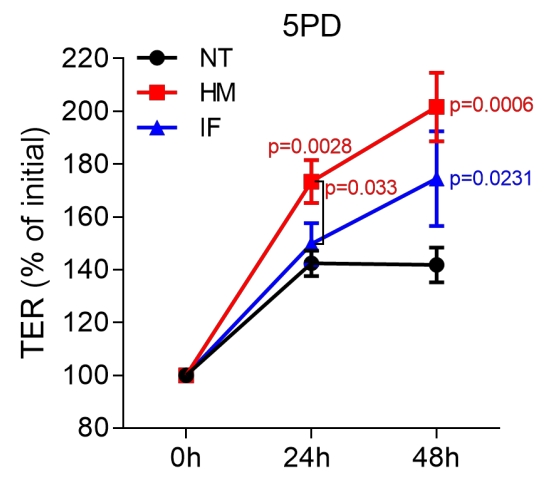
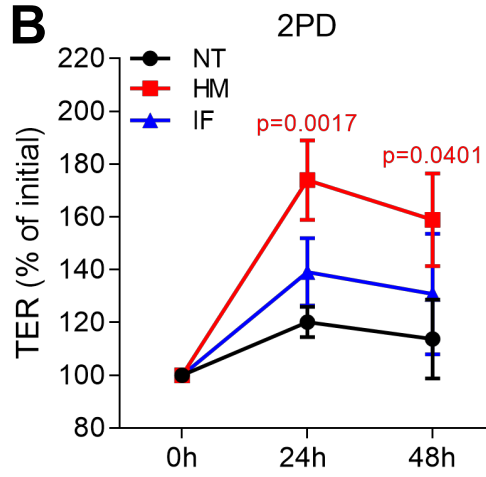
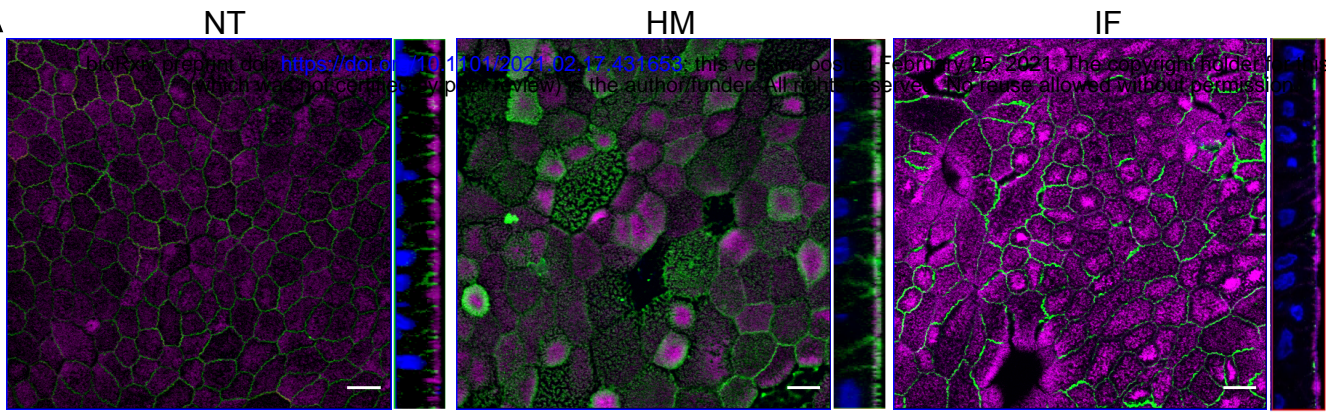
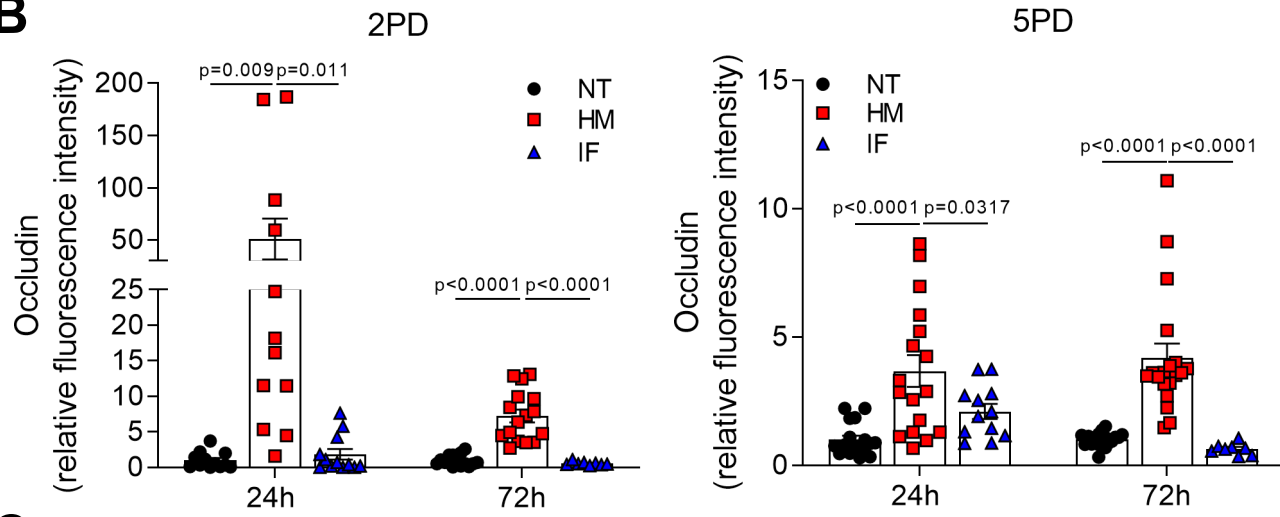


# Figure 3

**A**



**B**



**C**

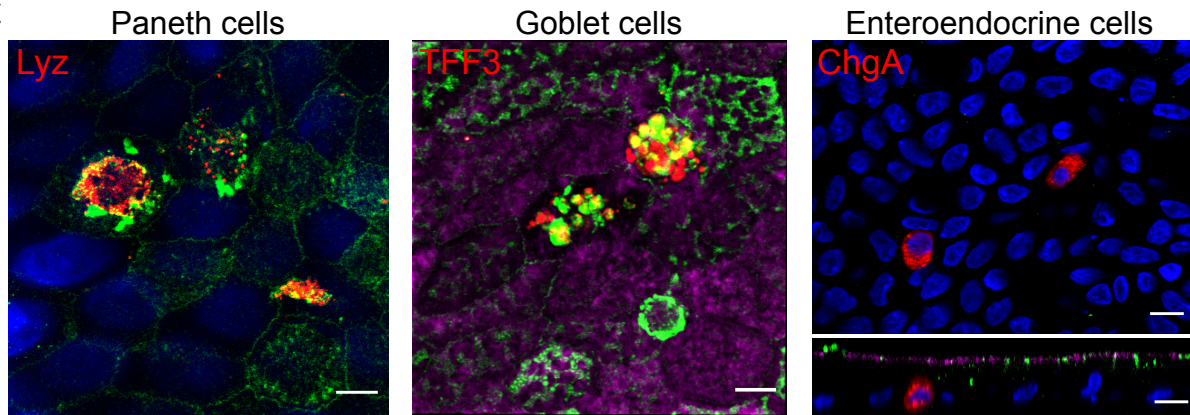


# Figure 4

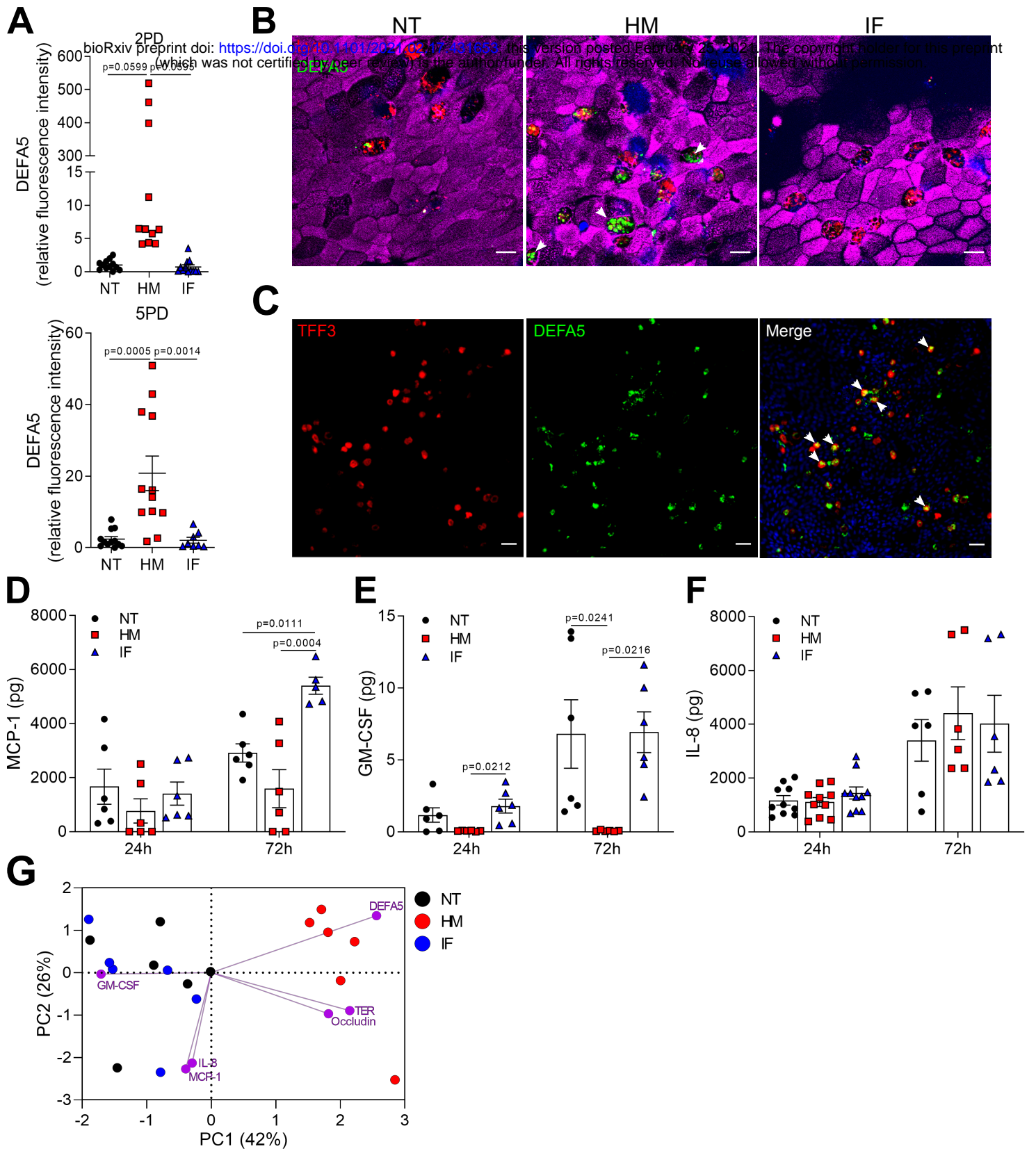


# Figure 5

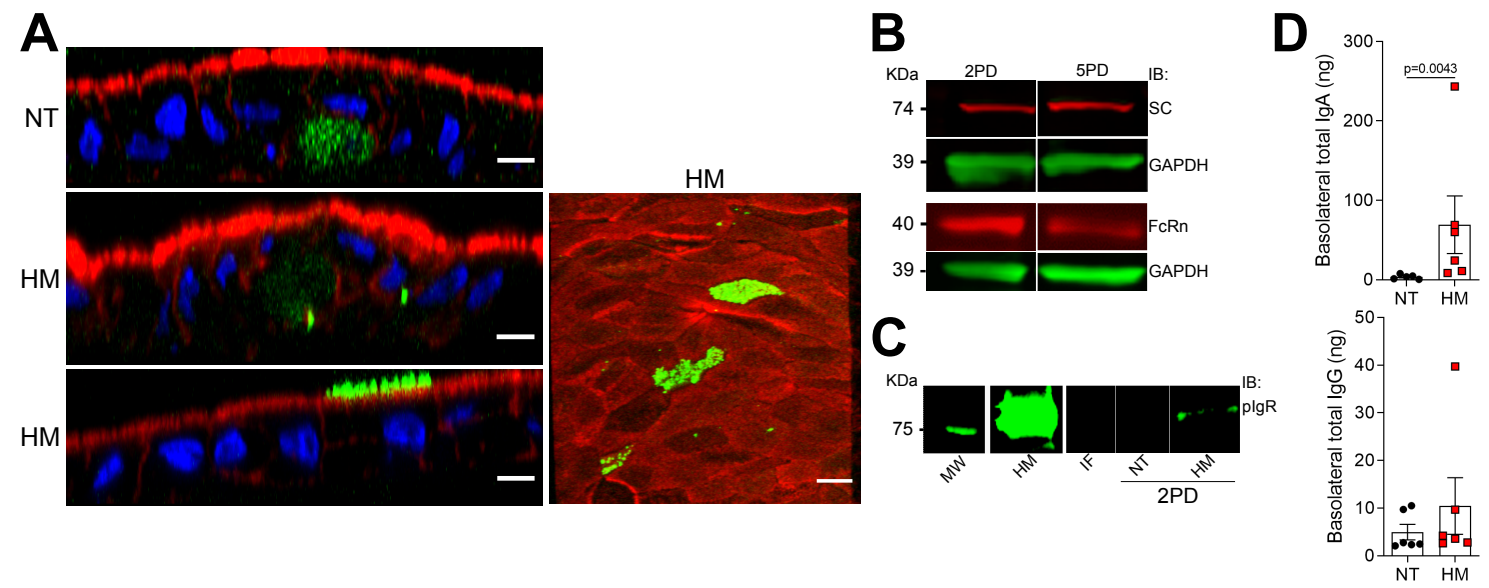




# Figure 6

